The long-run welfare impact of hydrological extremes in sub-Saharan Africa

Ahmed T. Hammad[1,2] **and Giacomo Falchetta**[3,4,*]

[1]Department of International Economics, Institutions and Development, Catholic University of Milan, Italy
[2]Decatab Pte Ltd., Singapore
[3]Department of Economics, Ca' Foscari University of Venice, Venice, Italy
[4]International Institute for Applied Systems Analysis, Laxenburg, Austria
[*]Corresponding author's email address: falchetta@iiasa.ac.at

ABSTRACT

The economic impact of dry and wet spells is increasingly investigated, also relative to anthropogenic climate change. Combining high-resolution wealth estimates[1] and long-run (1901-2018) hydrological records[2] for nearly one million settlements , here we empirically estimate the long-run welfare impact of hydrological events in sub-Saharan Africa (SSA). To achieve causal identification, we adopt a generalised propensity score approach allowing for continuous longitudinal treatments. Our results suggest that hydrological events played a long-lasting impact in shaping the current wealth distribution patterns in SSA. While even moderate dry spells diminished wealth (on average -$110 in the local per-capita GDP for each additional dry month), only extreme wet spells show a significant impact, but this is significantly harsher (-$387). We examine the temporal variability of estimates and discuss the significance of adaptive capacity. Our findings support the consideration of adaptation investment to mitigate future impacts and an exacerbation of existing inequalities.

Keywords

Long-run climate impact; hydrological extremes; economic development; inequality; propensity score weighting

This paper is a non-peer reviewed preprint submitted to EarthArXiv.

Introduction

The role of climate and climate extreme events in shaping the current distribution of wealth across and within countries is a long-debated topic[3–7]. The issue has become even more relevant in the context of estimating the current and future economic impact of anthropogenic climate change[8,9]. This research strand has generally exploited empirically estimated parametric damage functions which link temperature and other climate factors with macroeconomic outcomes[10–13]. Other ex-post climate impact evaluation studies have focused on specific sectors, such as agriculture[14,15] or labour productivity[16,17].

Yet, most empirical evaluations connecting climate and economic outcomes have been carried out at large levels of aggregation such as at the country level[4,18], or across sub-national administrative units[19]. While useful to understand global cross-country and regional dynamics, these assessments however hide inequalities and smooth out the local determinants of the observed levels and distribution of wealth. These local factors include climate indicators, but also specific geographic, socio-demographic, and institutional factors.

Building on novel non-conventional wealth estimates[1], long-run historical climate[20] and hydrological events (dry and wet spells)[2] records, and a broad set of socio-demographic, geographic, natural resource, environmental and institutional covariates, here we estimate the long-run welfare impact of drought and flood events incidence measured through the Standardised Precipitation Evapotranspiration Index (SPEI) in the period 1901-2018 in sub-Saharan

Africa. Our analysis benefits from a high spatial high-resolution (2.4 km) covering a large number of settled locations (n=911,430) across 42 countries of sub-Saharan Africa.

In our study, treatment variables are defined as the count of moderate (SPEI $\pm$ 1.5) and extreme (SPEI $\pm$ 2) dry or wet spells (see Materials and Methods) over four periods: 1901-1928, 1929-1958, 1959-1988, and 1989-2018. The use of such time windows allows for instance to differentiate the impact of early 20th century climate from that of more recent decades. Nonetheless, the approach is still suitable to estimate the cumulative treatment effect over the four treatment periods of interest. A detailed visualisation of the density distribution of the dry and wet moderate and extreme events in the time period under analysis is found in Figures SI-1 - SI-3.

In addition, to offer a visual representation of the distribution and spatial heterogeneity in the data, Figure 1 illustrates the two wealth outcome variables (the RWI, Relative Wealth Index, and the AWE, Absolute Wealth Estimate; see Materials and Methods) and two of the four treatment variables (the counts of moderate dry and wet spell months, see Materials and Methods for details) considered in this study.

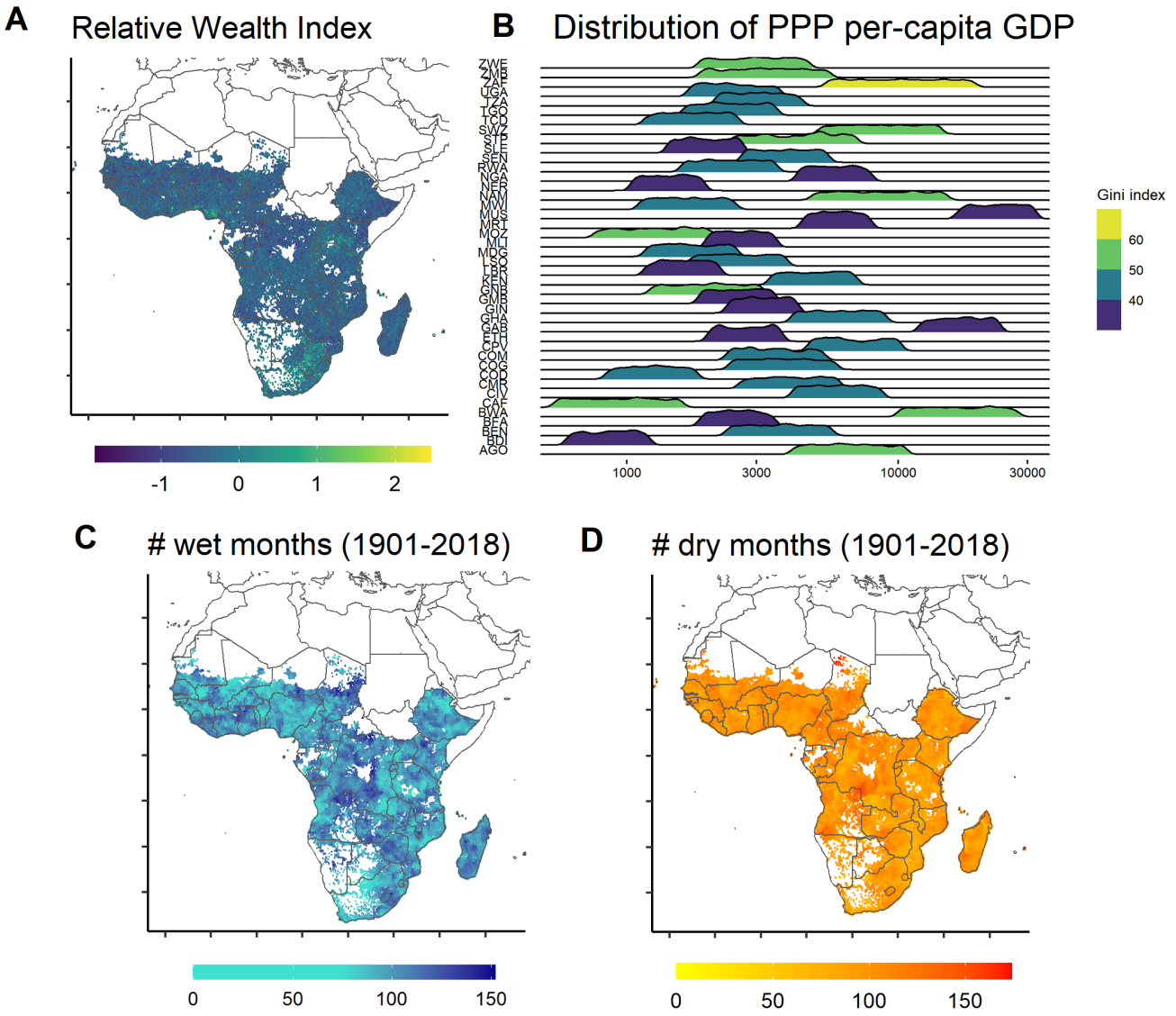

Figure 1. (A) Spatial distribution of the relative wealth index (RWI) in sub-Saharan Africa[1]; (B) Ridgeline plot for the within and across country distribution of the Absolute Wealth Estimate (AWE, see Materials and Methods for calculation detail). The colour fill mirrors the national Gini index; (C,D) Maps of the cumulative count of months classified as wet and dry spells (SPEI $\pm$ 1.5,[2]) respectively, in the 1901-2018 period.

The econometric identification strategy adopted is schematically represented in the framework of Figure 2. Namely, to ensure a causal identification of the welfare impact of hydrological events, we adopt a generalised propensity score (GPS) matching approach[21,22] within a marginal structural model for time-varying treatments[23] (see Materials and Methods for a detailed description of the methodology and of the underlying data). Weights are used to balance a broad set of socio-demographic, geographic, natural resource, environmental and institutional covariates and dealing with potential confounding factors in the relation between wealth and hydrological events incidence. The goal of the procedure is to generate appropriate balancing weights that ensure independence between the treatment variables and the set of covariates.

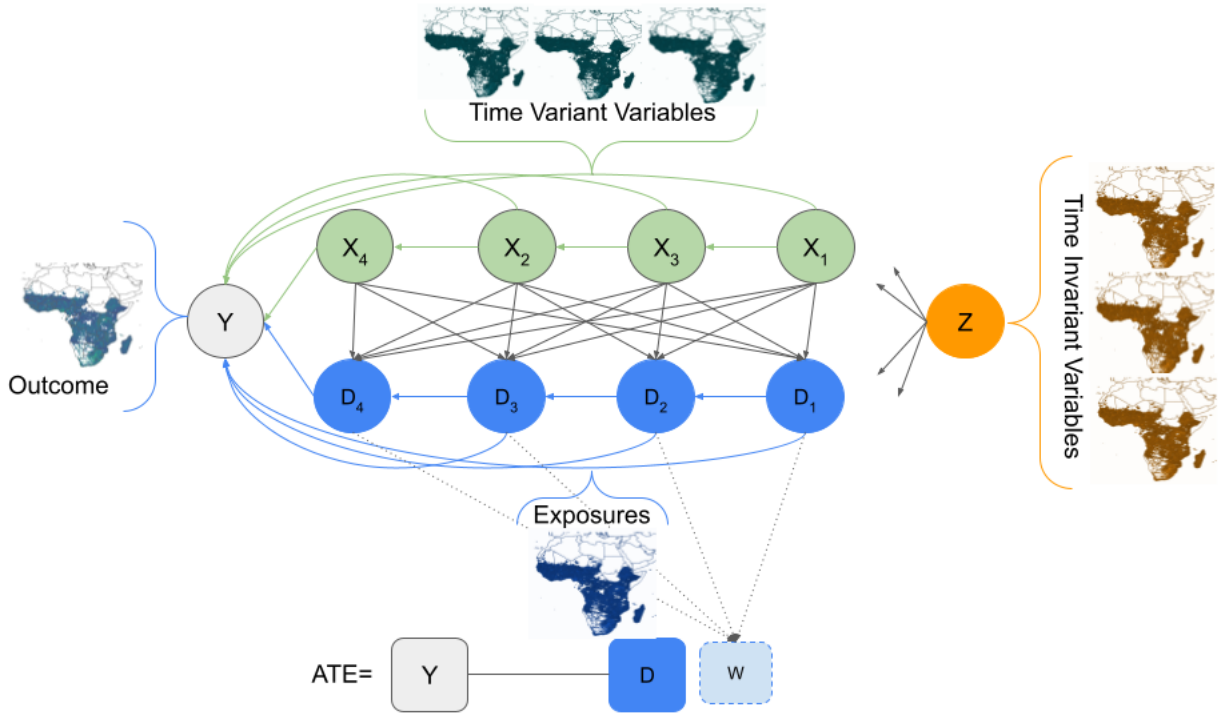

Figure 2. Framework for the identification strategy adopted in this paper. *Y* is the outcome. *Z* represents a set of time invariant covariates (or baseline covariates). *D* is a set of exposures at different points in time (1=1901 - 1928, 2=1929 - 1958, 3=1959 - 1988, 4=1989 - 2018). *X* represent the set of time variant covariates that affect the exposure and the outcome. We use a marginal structural model for time-varying treatments to take in account the temporal order of exposure and confounders (both time variant and time invariant). *Note*: **Y**: wealth micro-data[24]; **D**: SPEI events counts[2] (see Materials and Methods); **(X,Z)**: time variant and time invariant covariates (see Data section in the Materials and Methods for a detailed account); **w**: GPS weights.

Materials and Methods

Data

The key outcome variable of the analysis is based on novel satellite-based and survey-validated wealth micro-data[24]. The non-conventional wealth data come with a resolution of 2.4 km, covering 42 countries for a total of 911,430 settlements. Convolutional neuronal networks (CNN) are used to train a model with several satellite data products and produce estimates for unsurveyed settlements. The publicly available data product includes the Relative Wealth Index (RWI) variable. This index is calculated taking the first principal component of the answers from a standardized set of questions about assets and housing characteristics derived from DHS surveys[24,25]. To derive an outcome variable in monetary units, we convert this RWI into an Absolute Wealth Estimate (AWE), as discussed in the Absolute Wealth Estimate calculation section below. Treatment variables and covariates are then extracted within the same areal unit of each settlement in the wealth estimate dataset.

Our treatment of interest is given by counts of hydrological events over four time windows of about thirty years each, i.e. 1901-1928, 1929-1958, 1959-1988, and 1989-2018. We adopt the Standardized Precipitation Evapotranspiration Index (SPEI) obtained from the global SPEI Database (https://spei.csic.es/spei_database). In the context of our analysis we consider the monthly SPEI at a time-scale of 24 months (SPEI-24), namely accounting for the accumulated (rolling) deficit/oversupply over the previous two year at each month. As discussed in the literature[26], a SPEI time-scale of 24 months is deemed the most appropriate for evaluations of the socio-economic consequences of hydrological events like droughts and floods.

In addition, we control for average local climate conditions by processing precipitation, temperature and wetness time-series from the CRU TS v. 4.05 database[20]. The average climate conditions are extracted for the same time

windows of the SPEI treatment variables to account for changing climate normals over the periods in question.

Population count and degree of urbanisation (DoU) data are drawn from the Global Human Settlement Layer products suite[27,28], produced by the European Commission Joint Research Center. We refer to the 2019 revision of the two data products. We convert the categorical degree of urbanisation data into a binary urban-rural mask, considering DoU values >=20 as urban grid cells. We retrieve the *simplemaps* World Cities Database https://simplemaps.com/data/world-cities and use cost-based accessibility algorithms offered by the *accCost* function in the *gdistance* R package in combination with recent motorised transport friction layers[29] to estimate the average travel time to the nearest city from each grid cell.

In addition, we calculate the Malaria Stability Index[30] at each location, as well as the prevalent agro-ecological zone[31], and the proportion of area which is covered by cropland and forests, respectively[32].

We also consider the PRIO-GRID 2.0 database[33] to process a number of additional spatially-explicit covariates, including the distance to the capital city, the distance to the nearest country and the distance from the own boundaries, as well as the local availability of diamonds, gold, petroleum or gems.

Finally, we process information about altitude from the GTOPO30 global digital elevation model[34], based on which we also estimate the slope in Google Earth Engine.

When it comes to country-level covariates, we extract the most recent available statistics from the World Bank Data (https://data.worldbank.org/) for each country on the country urbanisation level, land area, hectares of agricultural land per capita, electricity access level, the rate of kids enrolment in primary schools, the amount of renewable freshwater resources per capita, the ease of doing business index, the average time to start a business, the index of institutional quality in the public sector management, the index of social inclusion policies, the index of legal rights strengths, the GDP share of energy imports and fuel and ores and metals exports.

SPEI index processing

In our study, treatment variables are defined as the count of dry or wet spell events (see Materials and Methods) over four periods: 1901-1928, 1929-1958, 1959-1988, and 1989-2018.

For each time window we define four variables:

- Two variables for the count of months where the SPEI index is $\pm$ 1.5, defined as moderate hydrological events; positive values of the SPEI index denote wet spells, while negative values refer to dry spells.
- Two variables for the count of months where the SPEI index is $\pm$ 2, defined as extreme hydrological events.

Thus, extreme events are defined as a subset of the count of moderate events. Figures SI-1-SI-3 in the SI Appendix show the density distributions of the values of these treatment variables for each of the four time windows considered.

Absolute Wealth Estimate calculation

As discussed above, the non-conventional wealth data considered come as a RWI based on assets and housing characteristics derived from DHS surveys. The main disadvantage of the RWI is that the values at each settlement i express the wealth level relative to other settlements in the same country c, making it not directly usable for cross-country analysis.

Following the Materials and Methods described in[24] itself, we use the approach of[35] to estimate the absolute wealth of households (AWE) based on the rank of the RWI and the assumed shape of the distribution of wealth among a national population. Our AWE is a measure of the average per-capita GDP (in 2011 PPP USD) of households located in each settlement contained in the orignal RWI data, and it is comparable across countries.

In particular, to estimate the AWE a log-normal distribution is parametrised with $\mu_c = \log(gdpcapita_c) - \frac{sd^2}{/2}$ and $sd_c = \sqrt{2} \times probit(\frac{gini_c+1}{/2})$ where c is each country, while *gini* and *gdpcapita* are the Gini index and the PPP per-capita GDP (2011 USD) for the most recent year available in the World Bank database[36].

The distribution of the RWI and AWE variables in each country is mapped in Figure SI-5 in the SI Appendix.

Identification strategy: covariates balancing at the settlement level

We frame the estimation of the joint causal effect of each treatment period on the two measures of wealth as a marginal structural model for time-varying treatments[23]. First, we estimate the General Propensity Score (GPS) balance weights at each treatment period following[21], using the rich set of time-invariant covariates and any other time-varying covariate from the current and the previous periods discussed in the Data section above.

The goal is to balance all the variables measured prior to a given treatment time point, accounting for all previous treatments. Then, we generate a single set of weights as the product of each period's weights. The GPS can be estimated using GLM regression or a non-parametric model [1] The estimated coefficients and residual variance are used to define the density function of the conditional distribution of the treatment variable.

We use the following mathematical notation: let N denote the study sample size and J the number of periods considered. For each unit $i \in \{1,...,N\}$ at each period $j \in \{1,...,J\}$, let Z_i denote a set of time-invariant variables, X_{ij} the set of time-variant variables, D_{ij} denote the observed exposure for unit i at time j, Y_i denotes the observed outcome for unit i; and $Y_{ij}(w)$ denote the counterfactual outcome for unit i at the exposure level d. $f_{D_{ij}|Xij,Zi}(d|x,z)$, denote the general assignment mechanism defined as the conditional density of the exposure given the time-variant and time-invariant covariates at a given time, that is the GPS. To account for the effect of covariates and exposures in the previous periods (if any) we define a marginal structural model with multiple equations to take in account the temporal order of exposure and confounders as in Equation 1. The final set of weights is the product of all the GPS $\Pi_{j=1}^{J} t$.[2].

$$\begin{aligned} D_{ij=1} &= X_{ij=1} + Z_i \\ D_{ij=2} &= X_{ij=2} + X_{ij=1} + D_{ij=1} + Z_i \\ D_{ij=3} &= X_{ij=3} + X_{ij=2} + X_{ij=1} + D_{ij=2} + D_{ij=1} + Z_i \\ D_{ij=4} &= X_{ij=4} + X_{ij=3} + X_{ij=2} + X_{ij=1} + D_{ij=3} + D_{ij=2} + D_{ij=1} + Z_i \end{aligned} \tag{1}$$

We use two model specifications for the GPS, namely, GLM and Bayesian Additive Regression Trees (BART)[38–40]. We asses the goodness of the generated balancing weights using the Spearman Correlation Coefficient. The framework is implemented in the *WeightIt* R package[41]. A similar approach is found in[42].

Impacts estimation

To estimate the effects based on the calculated scoring weights, we use the survey-weighted generalized linear model (svyglm) function from the survey package to fit the model[43,44]. All statistical analyses were performed using R 4.0 (R Foundation for Statistical Computing, Vienna, Austria).

The model described in Equation 2 is used to estimate the joint causal effect of each treatment period j on the two measures of wealth for the two outcome variables of interest (the AWE and the RWI). Observations are weighted by the corresponding product of the GPS.

$$AWE_i/RWI_i = \alpha_i + \sum_{J}^{j=1} \beta_j \times D_{ij} \tag{2}$$

Then, to calculate the cumulative impact we sum the individual treatment periods in one single cumulative exposure following[45].

Robustness checks

As a robustness check, we provide alternative model specification for the GPS and for the impact estimation. For the former we used the Bayesian additive regression trees (BART) algorithm[46] as an alternative to GLM and compared

[1] For an excellent introduction to the Generalised Propensity Score the reader can refer to[37].

[2] We assume the conditional density to be normally distributed, except for the GPS of *dry extreme events*, where we used a kernel density estimation due to the non-generalizable distribution (see figure SI-2)

the number of balanced variables. For the latter, we fit a modified BART that features the inclusion of the estimated GPS (based on GLM) in the full set of covariates[47].

Table SI-2, shows how - contrarily to the GLM balancing reported in the Results section - BART does not achieve full balancing, albeit only on the *Dry-Extra* treatment. For this outcome variable, almost half of the variables have a correlation higher than 0.05 with the treatment even after the balancing procedure.

Finally, to examine the heterogeneity and robustness of the estimated effects at different levels of treatment intensity, we classify each of the four treatment variables into deciles and run the same second stage estimation as in equation 1. Plots SI-6 to SI-9 visually display the average effect at each decile of the treatment variables. The reuslts are particularly consistent for moderate dry events and extreme wet events, highlighting the detrimental effect of the number of events on wealth. On the other hand, the number of extreme dry events do not suggest clear significant effects on the outcome variable, while the number of moderate wet events seems may have a positive effect on the measure of wealth.

Results

Figure 3 and Table 1 present the results of the balancing procedure via linear regression. Covariates include both time-variant climate records (moving averages of precipitations, temperature and wetness for the same periods of the treatment), and current geographic (accessibility, altitude, distance to boundaries, malaria stability, cropland and forest cover), socio-demographic (population, urbanisation), economic (availability of natural resources) and institutional quality factors. The results show that the GPS balancing procedure is successful for all treatment variables considered. Namely, pre-balancing non-zero Spearman correlations are observed between covariates and the treatments, while - due to the GPS weighting - post-balancing all correlation coefficients converge to below 0.05. As a robustness check, we also implement the balancing procedure through a Bayesian Additive Regression Trees (BART) approach, see SI Appendix. Residual concerns - such as the omission of relevant covariates - are highlighted in the Discussion section. These concerns are however at least partly mitigated by the large number of covariates included and the large sample size.

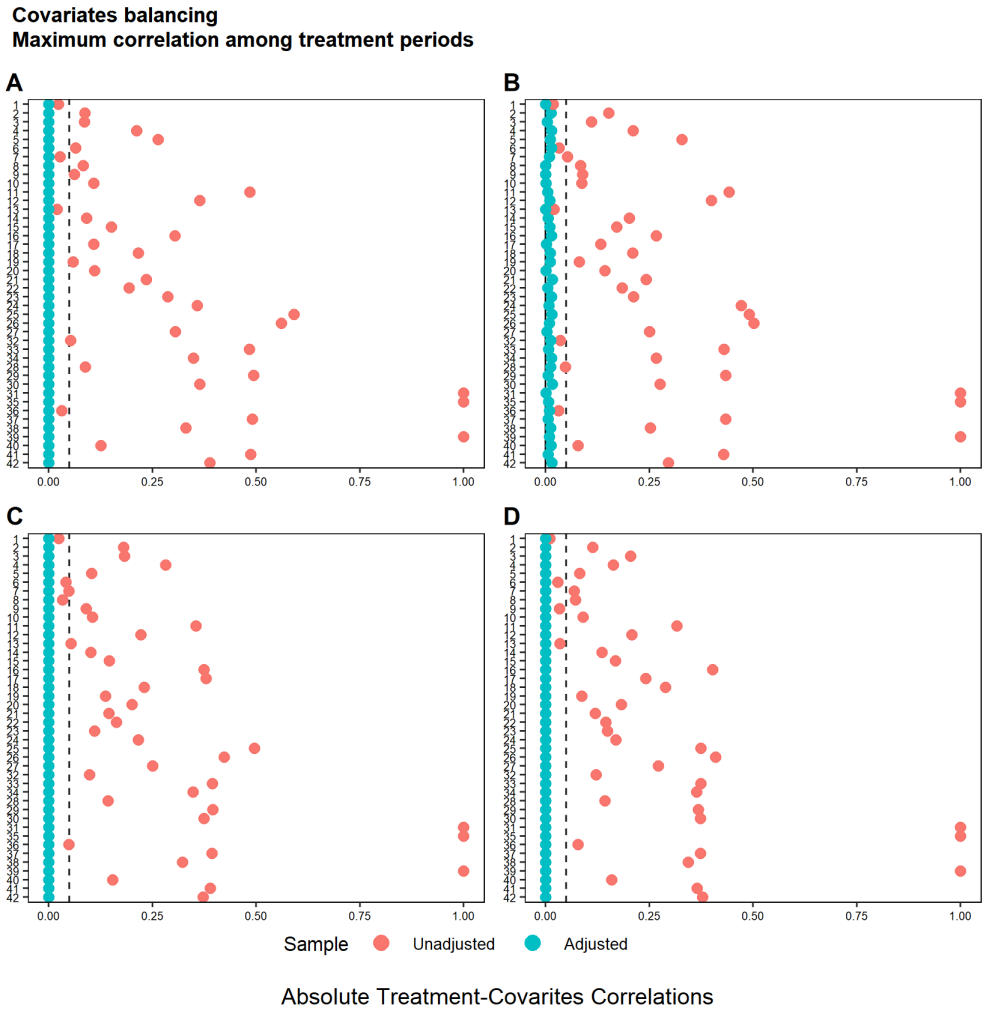

Figure 3. Results of the generalised propensity score (GPS) balancing procedure: Spearman correlation coefficients between treatment variables and balancing covariates. (A) moderate dry spells; (B) extreme dry spells; (C) moderate wet spells; (D) extreme wet spells. The ID numbers on the y-axis identify each covariate considered: a dictionary of each covariate is found in Table SI-SI-1. NB: country fixed effects are omitted from the chart but included in the balancing (i.e. they are included in the variable counts in Table 1.

Table 1. Covariates balancing summary: count of variables with a correlation coefficient ± 0.05 pre/post-balancing.

Pre-balancing				
	Dry	Dry-Extra	Wet	Wet-Extra
Balanced, <0.05	18	22	19	24
Not Balanced, >0.05	81	77	80	75
Post-balancing				
	Dry	Dry-Extra	Wet	Wet-Extra
Balanced, <0.05	99	99	99	99
Not Balanced, >0.05	0	0	0	0

Table 2. Cumulative impact of hydrological extremes on the RWI and AWE in sub-Saharan Africa

	Dependent variable:							
	RWI (dry)	AWE (dry)	RWI (dry extreme)	AWE (dry extreme)	RWI (wet)	AWE (wet)	RWI (wet extreme)	AWE (wet extreme)
	(1)	(2)	(3)	(4)	(5)	(6)	(7)	(8)
Cumulative # events	-0.008^{***}	-110.372^{***}	-0.004	-7.323	-0.003^{**}	-2.664^{***}	-0.025^{***}	-386.768^{***}
	(0.0003)	(19.565)	(0.003)	(5.319)	(0.001)	(0.869)	(0.003)	(47.183)
Constant	1.054^{***}	$20,705.330^{***}$	-0.156^{*}	$3,315.066^{***}$	-0.081	$2,412.524^{***}$	0.754^{***}	$21,357.310^{***}$
	(0.034)	(3,327.618)	(0.092)	(258.252)	(0.144)	(53.162)	(0.122)	(1,957.162)
Observations	911,430	911,430	911,430	911,430	911,430	911,430	911,430	911,430
Log Likelihood	-24,899,401.000	-34,458,531.000	-3,391,910.000	-11,375,114.000	-26,720,366.000	-32,104,980.000	-10,189,004.000	-19,017,967.000
Akaike Inf. Crit.	49,798,806.000	68,917,066.000	6,783,824.000	22,750,233.000	53,440,737.000	64,209,965.000	20,378,012.000	38,035,937.000

Note: *p<0.1; **p<0.05; ***p<0.01

Table 3. Time heterogeneity in the impact of hydrological extremes on the RWI and AWE in sub-Saharan Africa

	Dependent variable:							
	RWI (dry)	AWE (dry)	RWI (dry extreme)	AWE (dry extreme)	RWI (wet)	AWE (wet)	RWI (wet extreme)	AWE (wet extreme)
	(1)	(2)	(3)	(4)	(5)	(6)	(7)	(8)
# events (1901 - 1928)	-0.026^{***}	-255.935^{***}	-0.005^{*}	-1.400	-0.005^{***}	-18.369^{***}	-0.050^{***}	-708.612^{***}
	(0.001)	(70.210)	(0.003)	(8.005)	(0.001)	(3.186)	(0.006)	(101.464)
# events (1929 - 1958)	-0.014^{***}	-62.502	-0.024^{***}	-51.817^{*}	-0.001	30.703^{***}	-0.023^{***}	-556.895^{***}
	(0.001)	(61.576)	(0.007)	(31.259)	(0.001)	(3.144)	(0.004)	(63.225)
# events (1959 - 1988)	-0.014^{***}	-176.888^{***}	-0.004	-12.593^{**}	-0.001	51.815^{***}	-0.026^{***}	-366.127^{***}
	(0.0004)	(32.658)	(0.004)	(5.159)	(0.001)	(2.740)	(0.002)	(36.977)
# events (1989 - 2018)	-0.008^{***}	-110.371^{***}	-0.002	15.621	-0.007^{***}	-62.863^{***}	-0.021^{***}	-287.030^{***}
	(0.0003)	(19.564)	(0.002)	(10.956)	(0.002)	(3.306)	(0.002)	(37.210)
Constant	1.054^{***}	$20,705.330^{***}$	-0.145	$3,434.217^{***}$	-0.081	$2,412.524^{***}$	0.754^{***}	$21,357.310^{***}$
	(0.034)	(3,327.618)	(0.091)	(263.537)	(0.144)	(53.162)	(0.122)	(1,957.162)
Observations	911,430	911,430	911,430	911,430	911,430	911,430	911,430	911,430
Log Likelihood	-24,899,401.000	-34,458,531.000	-3,383,886.000	-11,359,798.000	-26,720,366.000	-32,104,980.000	-10,189,004.000	-19,017,967.000
Akaike Inf. Crit.	49,798,812.000	68,917,072.000	6,767,782.000	22,719,607.000	53,440,743.000	64,209,971.000	20,378,018.000	38,035,943.000

Note: *p<0.1; **p<0.05; ***p<0.01

The regression results suggest that while even moderate drought events have negatively impacted local wealth (an average -$110 decrease in the local GDP per capita for each additional dry spell month), only extreme wet events have exerted a negative impact on local wealth, but this is significantly harsher (-$387 for each additional extreme wet spell month). On the other hand, results for extreme dry events and mild wet events are less robust or significant in magnitude.

Interestingly, we find that the magnitude of the adverse impacts has decreased with time. Different potential factors might have driven this change in sensitivity to hydrological events, such as technology adoption, planning, and adaptation actions[48,49]. The Discussion Section elaborates further on these potential explanatory channels. Yet, it remains beyond the scope of this paper to explicitly investigate the role of adaptation.

Then, to summarise the results and jointly compare them, Figure 4 visualises the estimated marginal effects (with 95% confidence intervals) of hydrological events on wealth, for both dry and wet and both moderate and extreme events. The x-axis show the four treatment periods and the four types of treatments in panels A and B, respectively, while the y-axes describe the average marginal effect of on additional dry or wet spell month on the AWE.

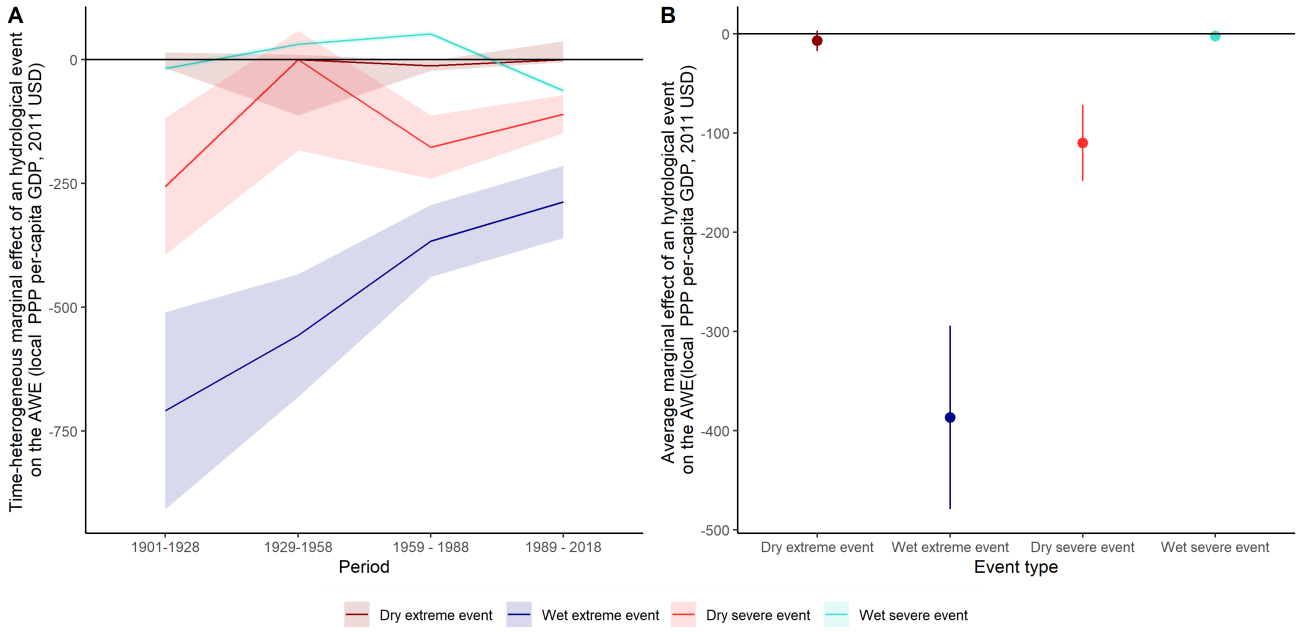

Figure 4. (A) Temporal evolution of the marginal effect of dry and wet moderate and extreme hydrological events on the observed absolute wealth estimate (AWE) estimate. (B) Average treatment effect on the AWE for each hydrological event category. Confidence intervals refer to $p = 95\%$.

To examine the heterogeneity and robustness of the estimated effects at different levels of treatment intensity, we also transform the treatment variables in a set of categorical variables based on the decile distribution. Regression results are reported in the SI Appendix. The analysis reveals how the welfare impact of the considered hydrological events varies across settlements that have experienced different (cumulative) levels of hydrological events incidence. The results of this supplementary analysis (Figures SI-6 - SI-9) suggest that there is a substantial and significant difference from the first decile and the rest of the distribution for moderate dry events, moderate wet events and extreme wet events. In particular, the effect of the number of wet events on AWE differ from the main regression results (table 2), suggesting that, to a certain extent, moderate wet events may have positive impact on wealth. On the other hand, the number of extreme dry events does not seems to have a clear and significant effect on AWE.

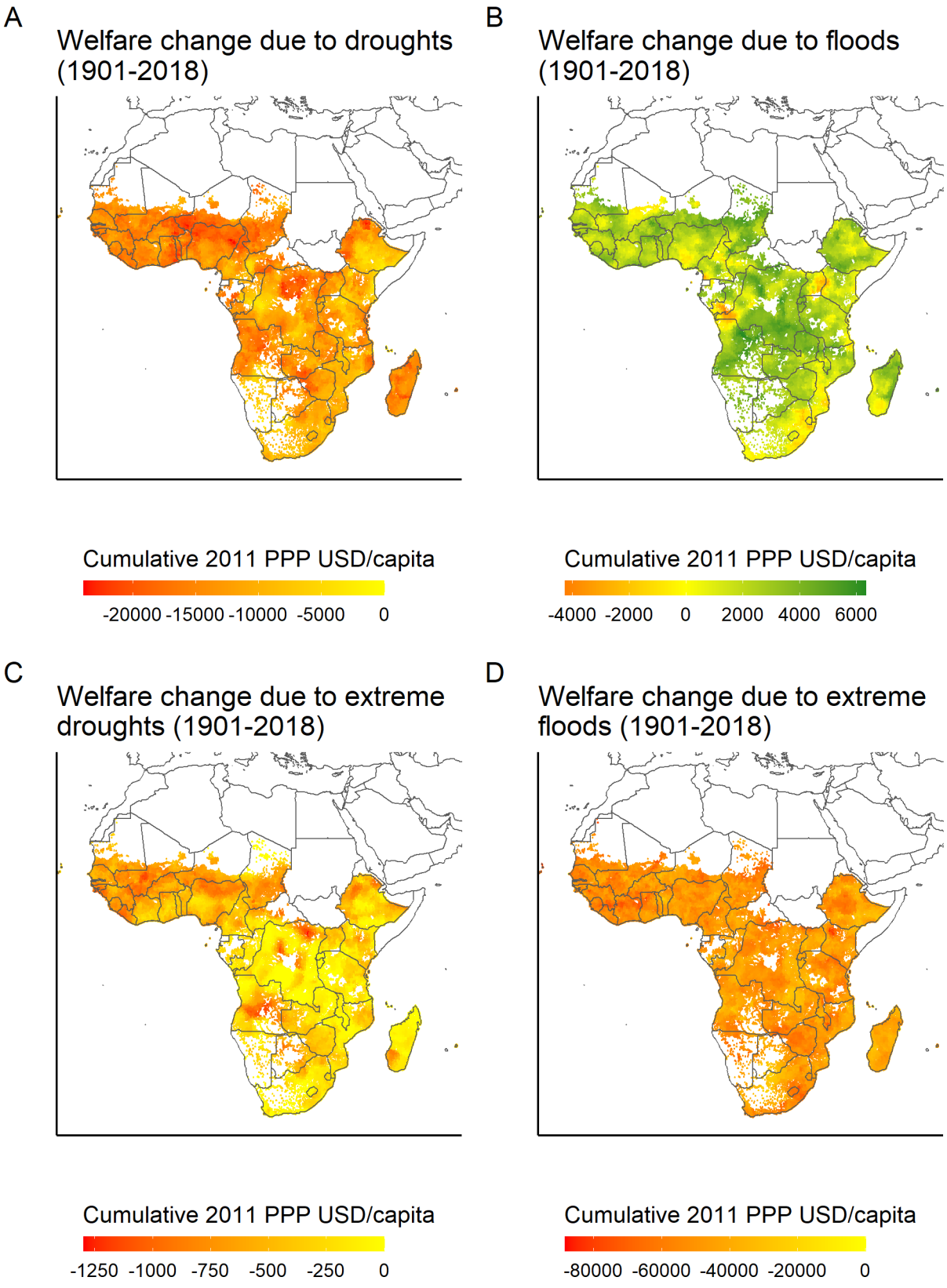

Figure 5. Maps of the long-run cumulative estimated welfare change (measured based on the AWE, in 2011 PPP USD/capita) for the 1901-2018 period due to: (A,B) moderate dry and wet events (C,D) extreme dry and wet events. Estimates are based on the statistically-significant (at $p < 0.05$) time-period and hydrological event type-specific coefficients and on the long-run record of incidence at each settlement in the dataset.

The maps reveal the variability in the incidence of hydrological events over different areas of sub-Saharan Africa, as well as the heterogeneous welfare response across the different treatment variables. As discussed above, at lower levels of the $||SPEI||$, the welfare impact is larger and more significant for dry events. In particular, moderate wet events seem to also have partially benefited large areas, although with a rather small cumulative magnitude, considering the nearly 120-year period in question. On the other hand, at $||SPEI|| > 2$, the negative impact becomes significantly harsher for wet events. Hotspots of negative impact are found in the Sahel region, Zambezi valley, Northern Congo, and Magagascar, whilst areas where the impact of extreme wet events has been particularly adverse include areas of West Africa, northern Kenya, Zimbabwe, and eastern South Africa.

Discussion

Our analysis on the impact of hydrological extremes on the current observed levels of wealth in sub-Saharan Africa shows a significant long-run effect of both wet and dry hydrological events. In particular, we highlight that while even moderate dry events have negatively impacted local wealth (an average -$110 decrease in the local GDP per capita for each additional month of dry spell), only extreme wet spells are found to have exerted a negative impact on local wealth (on average, -$387 for each additional month of wet spell).

In most cases, the magnitude of the impact coefficients is found to have decreased with time across the four treatment periods. This finding implies that recent hydrological events have exerted a relatively milder impact to local wealth level compared to events farther in the past. An open question thus concerns the estimated decrease in the magnitude of the adverse welfare impact across the four 30-year periods between 1901 and 2018 considered in our analysis.

Whilst it remains beyond the scope of this paper to investigate these temporal patterns in detail, a potential explanatory channel may be a growing adaptive capacity through the gradual adoption of technology and of more resilient practices. This hypothesis is consistent with the findings of Ahmadalipour & Moradkhani[49], who carry out a multi-dimensional assessment of drought vulnerability in Africa for the 1960–2100 period. They find that between 1970-2015, drought vulnerability has decreased in many African countries, although with heterogeneous trends and some exceptions.

Another crucial finding to be linked with our analysis concerns the future drought vulnerability estimates reported in[49], who project increasing drought vulnerability. Climate change is and will in fact increasingly affect the frequency and intensity of extreme events over sub-Saharan Africa[50], albeit with significant uncertainty both over their magnitude and repercussions[51–53]. This suggests that a linear extrapolation based on our empirical estimates of the welfare impact of hydrological extremes in the past is not appropriate to estimate the potential future welfare loss caused by hydrological extremes. Future research could further investigate the patterns of accumulation of adaptive capacity stock in the region. Finally, an additional key open questions thus concern the evaluation of the optimal level of adaptation investment, as discussed in the relevant literature[54–57].

Overall, our study is the first of its kind to estimate the long-run welfare impact of drought and flood events incidence at high spatial high-resolution (2.4 km) and across a very large number of settled locations for a large region such as sub-Saharan Africa. The benefits of such granular and spatio-temporally detailed approach must however be considered together with some of the main potential limitations. First, the outcome variable of interest, i.e. the micro wealth estimates, are not exempt from error since they are produced with learning-based algorithms applied to satellite imagery (see[24]), which are validated against field survey data (which can themselves not always be unbiased; see https://dhsprogram.com/data/Data-Quality-and-Use.cfm). Similar arguments hold for long-term climate records upon which the CRU-TS and SPEI databases are built: uncertainty characterises both the *in-situ* observations used to validate the methodology (in particular those relating to the farthest years in the most data-sparse locations), and the underlying climate modelling to obtain spatio-temporally homogeneous observations (see[2,20]).

Besides the data limitations, also the methodology adopted to seek causal identification and estimate the direct impact of hydrological events on wealth is subject to potential sources of error. For instance, the cross sectional data and selection of co-variates for the GPS balancing still allow for potential concerns related to the omission of

variables correlated with both the local wealth estimates and the historical incidence of hydrological events. We sought to mitigate this concern with the inclusion of a broad set of covariates in the balancing procedure.

Bearing these potential limitations in mind, our analysis represents an innovative attempt to combine long-term historical vulnerability analysis with very granular spatial resolution data to evaluate the welfare impact of hydrological events in the sub-Saharan African region. Based on our findings, the main conclusion is that moderate dry spells and extreme wet spells seem to have played a strong and long-lasting impact in shaping today's patterns of wealth distribution in sub-Saharan Africa. Without sufficient adaptation investment, future extremes are likely to further exacerbate this inequality.

References

1. Chi, G., Fang, H., Chatterjee, S. & Blumenstock, J. E. Micro-estimates of wealth for all low- and middle-income countries (2021). 2104.07761.
2. Vicente-Serrano, S. M., Beguería, S., López-Moreno, J. I., Angulo, M. & Kenawy, A. E. A new global 0.5° gridded dataset (1901–2006) of a multiscalar drought index: Comparison with current drought index datasets based on the palmer drought severity index. *J. Hydrometeorol.* **11**, 1033–1043, DOI: 10.1175/2010jhm1224.1 (2010).
3. Karaca, O. Why are some regions rich and others poor? the impact of climate on regional income disparities. *Appl. Econ. Lett.* **27**, 353–356 (2020).
4. Burke, M., Hsiang, S. M. & Miguel, E. Global non-linear effect of temperature on economic production. *Nature* **527**, 235–239 (2015).
5. Lambert, L. D. The role of climate in the economic development of nations. *Land Econ.* **47**, 339–344 (1971).
6. Nordhaus, W. D. Climate and economic development: climates past and climate change future. *The World Bank Econ. Rev.* **7**, 355–376 (1993).
7. Gallup, J. L., Sachs, J. D. & Mellinger, A. D. Geography and economic development. *Int. regional science review* **22**, 179–232 (1999).
8. Tol, R. S. J. Do climate dynamics matter for economics? *Nat. Clim. Chang.* **11**, 802–803, DOI: 10.1038/s41558-021-01169-5 (2021).
9. Tol, R. S. The impacts of climate change according to the ipcc. *Clim. Chang. Econ.* **7**, 1640004 (2016).
10. Diaz, D. & Moore, F. Quantifying the economic risks of climate change. *Nat. Clim. Chang.* **7**, 774–782 (2017).
11. Hsiang, S. *et al.* Estimating economic damage from climate change in the united states. *Science* **356**, 1362–1369 (2017).
12. Botzen, W. W. & van den Bergh, J. C. How sensitive is nordhaus to weitzman? climate policy in dice with an alternative damage function. *Econ. Lett.* **117**, 372–374 (2012).
13. Auffhammer, M. Quantifying economic damages from climate change. *J. Econ. Perspectives* **32**, 33–52 (2018).
14. Antle, J. M. & Stöckle, C. O. Climate impacts on agriculture: insights from agronomic-economic analysis. *Rev. Environ. Econ. Policy* **11**, 299–318 (2017).
15. Mersha, F. & Leta, A. Climate change and its impact on agricultural production: an empirical review from sub-saharan african perspective. *J. Agric. Econ.* **5**, 627–633 (2019).
16. Zander, K. K., Botzen, W. J., Oppermann, E., Kjellstrom, T. & Garnett, S. T. Heat stress causes substantial labour productivity loss in australia. *Nat. climate change* **5**, 647–651 (2015).
17. Knittel, N., Jury, M. W., Bednar-Friedl, B., Bachner, G. & Steiner, A. K. A global analysis of heat-related labour productivity losses under climate change—implications for germany's foreign trade. *Clim. Chang.* **160**, 251–269 (2020).

18. Dell, M., Jones, B. F. & Olken, B. A. Temperature shocks and economic growth: Evidence from the last half century. *Am. Econ. Journal: Macroecon.* **4**, 66–95, DOI: 10.1257/mac.4.3.66 (2012).

19. Kalkuhl, M. & Wenz, L. The impact of climate conditions on economic production. evidence from a global panel of regions. *J. Environ. Econ. Manag.* **103**, 102360, DOI: 10.1016/j.jeem.2020.102360 (2020).

20. Harris, I., Osborn, T. J., Jones, P. & Lister, D. Version 4 of the CRU TS monthly high-resolution gridded multivariate climate dataset. *Sci. Data* **7**, DOI: 10.1038/s41597-020-0453-3 (2020).

21. Hirano, K. & Imbens, G. W. The propensity score with continuous treatments. *Appl. Bayesian modeling causal inference from incomplete-data perspectives* **226164**, 73–84 (2004).

22. Fong, C., Hazlett, C. & Imai, K. Covariate balancing propensity score for a continuous treatment: Application to the efficacy of political advertisements. *The Annals Appl. Stat.* **12**, 156–177 (2018).

23. Cole, S. R. & Hernán, M. A. Constructing inverse probability weights for marginal structural models. *Am. journal epidemiology* **168**, 656–664 (2008).

24. Chi, G., Fang, H., Chatterjee, S. & Blumenstock, J. E. Micro-estimates of wealth for all low-and middle-income countries. *arXiv preprint arXiv:2104.07761* (2021).

25. Measure, D. *et al.* Statcompiler. *Calverton, Maryland, USA* (2021).

26. Potop, V., Boroneanţ, C., Možnỳ, M., Štěpánek, P. & Skalák, P. Observed spatiotemporal characteristics of drought on various time scales over the czech republic. *Theor. applied climatology* **115**, 563–581 (2014).

27. Pesaresi, M., Florczyk, A., Schiavina, M., Melchiorri, M. & Maffenini, L. Ghs settlement grid, updated and refined regio model 2014 in application to ghs-built r2018a and ghs-pop r2019a, multitemporal (1975-1990-2000-2015), r2019a, DOI: 10.2905/42E8BE89-54FF-464E-BE7B-BF9E64DA5218 (2019).

28. Pesaresi, M., Florczyk, A., Schiavina, M., Melchiorri, M. & Maffenini, L. Ghs settlement grid, updated and refined regio model 2014 in application to ghs-built r2018a and ghs-pop r2019a, multitemporal (1975-1990-2000-2015), r2019a, DOI: 10.2905/42E8BE89-54FF-464E-BE7B-BF9E64DA5218 (2019).

29. Weiss, D. *et al.* Global maps of travel time to healthcare facilities. *Nat. Medicine* **26**, 1835–1838 (2020).

30. Kiszewski, A. *et al.* A global index representing the stability of malaria transmission. *The Am. journal tropical medicine hygiene* **70**, 486–498 (2004).

31. Fischer, G. *et al.* Global agro-ecological zones (gaez v4)-model documentation. (2021).

32. Buchhorn, M. *et al.* Copernicus global land service: Land cover 100m: collection 3: epoch 2019: Globe, DOI: 10.5281/ZENODO.3939050 (2020).

33. Tollefsen, A. F., Bahgat, K., Nordkvelle, J. & Buhaug, H. Prio-grid v. 2.0 codebook. *J. Peace Res.* **49**, 363–374 (2016).

34. Miliaresis, G. C. & Argialas, D. Segmentation of physiographic features from the global digital elevation model/gtopo30. *Comput. & Geosci.* **25**, 715–728 (1999).

35. Hruschka, D. J., Gerkey, D. & Hadley, C. Estimating the absolute wealth of households. *Bull. World Heal. Organ.* **93**, 483–490 (2015).

36. Group, W. B. The world bank data catalog (2021).

37. Austin, P. C. Assessing the performance of the generalized propensity score for estimating the effect of quantitative or continuous exposures on binary outcomes. *Stat. medicine* **37**, 1874–1894 (2018).

38. Chipman, H. A., George, E. I. & McCulloch, R. E. Bart: Bayesian additive regression trees. *The Annals Appl. Stat.* **4**, 266–298 (2010).

39. Hahn, P. R., Murray, J. S. & Carvalho, C. M. Bayesian regression tree models for causal inference: Regularization, confounding, and heterogeneous effects (with discussion). *Bayesian Analysis* **15**, 965–1056 (2020).

40. Hill, J., Weiss, C. & Zhai, F. Challenges with propensity score strategies in a high-dimensional setting and a potential alternative. *Multivar. Behav. Res.* **46**, 477–513 (2011).

41. Greifer, N. *WeightIt: Weighting for Covariate Balance in Observational Studies* (2021). R package version 0.12.0.

42. Mason, C., Sabariego, C., Thng, Đ. M. & Weber, J. Can propensity score matching be applied to cross-sectional data to evaluate community-based rehabilitation? results of a survey implementing the who's community-based rehabilitation indicators in vietnam. *BMJ Open* **9**, DOI: 10.1136/bmjopen-2018-022544 (2019). https://bmjopen.bmj.com/content/9/1/e022544.full.pdf.

43. Lumley, T. survey: analysis of complex survey samples (2020). R package version 4.0.

44. Lumley, T. Analysis of complex survey samples. *J. Stat. Softw.* **9**, 1–19 (2004). R package verson 2.2.

45. Robins, J. M., Hernan, M. A. & Brumback, B. Marginal structural models and causal inference in epidemiology (2000).

46. Chipman, H. A., George, E. I. & McCulloch, R. E. BART: Bayesian additive regression trees. *The Annals Appl. Stat.* **4**, DOI: 10.1214/09-aoas285 (2010).

47. Hill, J. L. Bayesian nonparametric modeling for causal inference. *J. Comput. Graph. Stat.* **20**, 217–240 (2011).

48. Osbahr, H., Twyman, C., Adger, W. N. & Thomas, D. S. Evaluating successful livelihood adaptation to climate variability and change in southern africa. *Ecol. Soc.* **15** (2010).

49. Ahmadalipour, A. & Moradkhani, H. Multi-dimensional assessment of drought vulnerability in africa: 1960–2100. *Sci. total environment* **644**, 520–535 (2018).

50. Arias, P. *et al.* Climate change 2021: The physical science basis. contribution of working group14 i to the sixth assessment report of the intergovernmental panel on climate change; technical summary. (2021).

51. Nangombe, S. *et al.* Record-breaking climate extremes in africa under stabilized 1.5 c and 2 c global warming scenarios. *Nat. Clim. Chang.* **8**, 375–380 (2018).

52. Tabari, H., Hosseinzadehtalaei, P., AghaKouchak, A. & Willems, P. Latitudinal heterogeneity and hotspots of uncertainty in projected extreme precipitation. *Environ. Res. Lett.* **14**, 124032 (2019).

53. AghaKouchak, A. *et al.* Climate extremes and compound hazards in a warming world. *Annu. Rev. Earth Planet. Sci.* **48**, 519–548 (2020).

54. Xu, T. *et al.* Optimal adaptation pathway for sustainable low impact development planning under deep uncertainty of climate change: A greedy strategy. *J. environmental management* **248**, 109280 (2019).

55. Klein, R. J. Adaptation to climate variability and change: what is optimal and appropriate. *Clim. Chang. Mediterr. Socio-Economic Perspectives Impacts, Vulnerability Adapt.* **32** (2003).

56. Rosbjerg, D. Optimal adaptation to extreme rainfalls in current and future climate. *Water Resour. Res.* **53**, 535–543 (2017).

57. Bosello, F., Carraro, C. & De Cian, E. Climate policy and the optimal balance between mitigation, adaptation and unavoided damage. *Clim. Chang. Econ.* **1**, 71–92 (2010).

SI: Appendix

Density Distribution of the Treatment variables

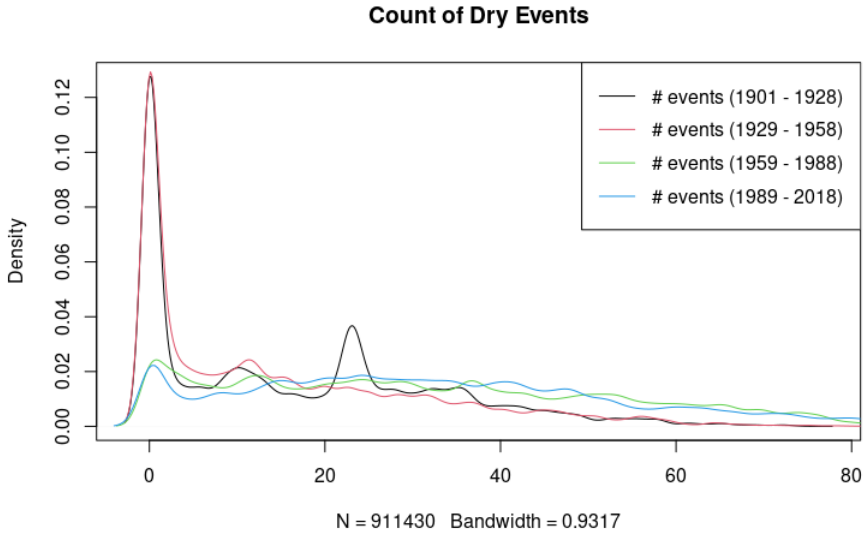

Figure SI-1. Density distribution of dry events (SPEI-24 < 1.5)

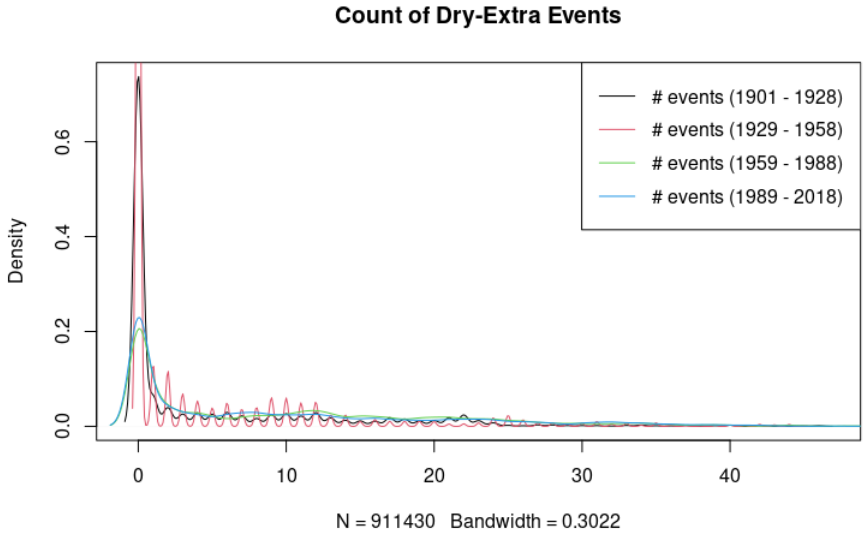

Figure SI-2. Density distribution of dry events (SPEI-24 < 2)

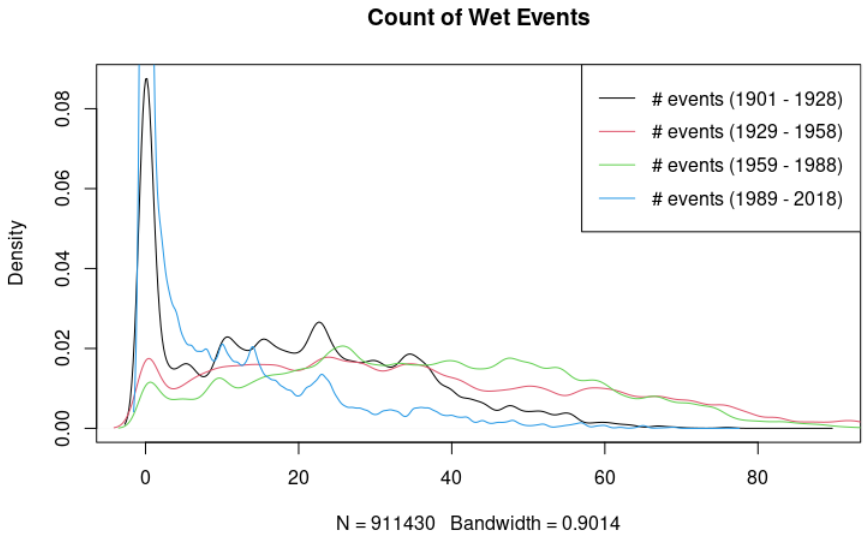

Figure SI-3. Density distribution of dry events (SPEI-24 $>$ 1.5)

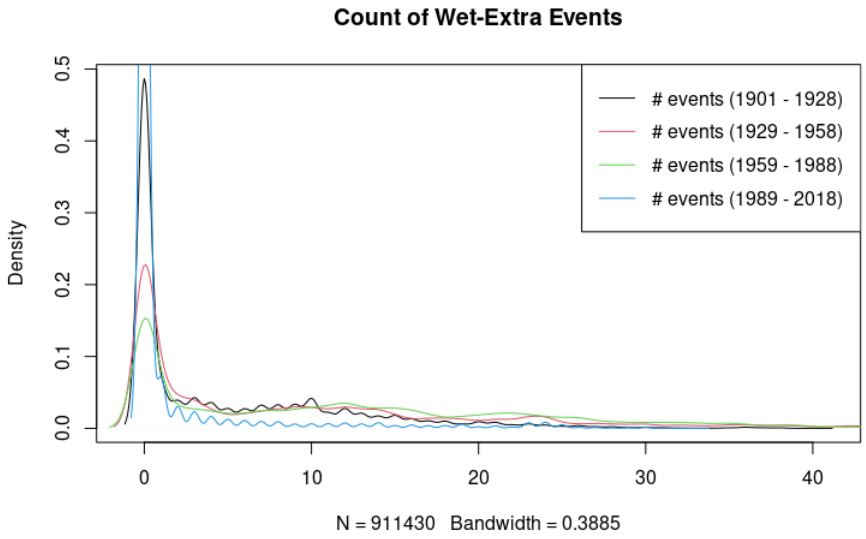

Figure SI-4. Density distribution of dry events (SPEI-24 $>$ 2)

Distribution of the RWI and AWE indicators across countries

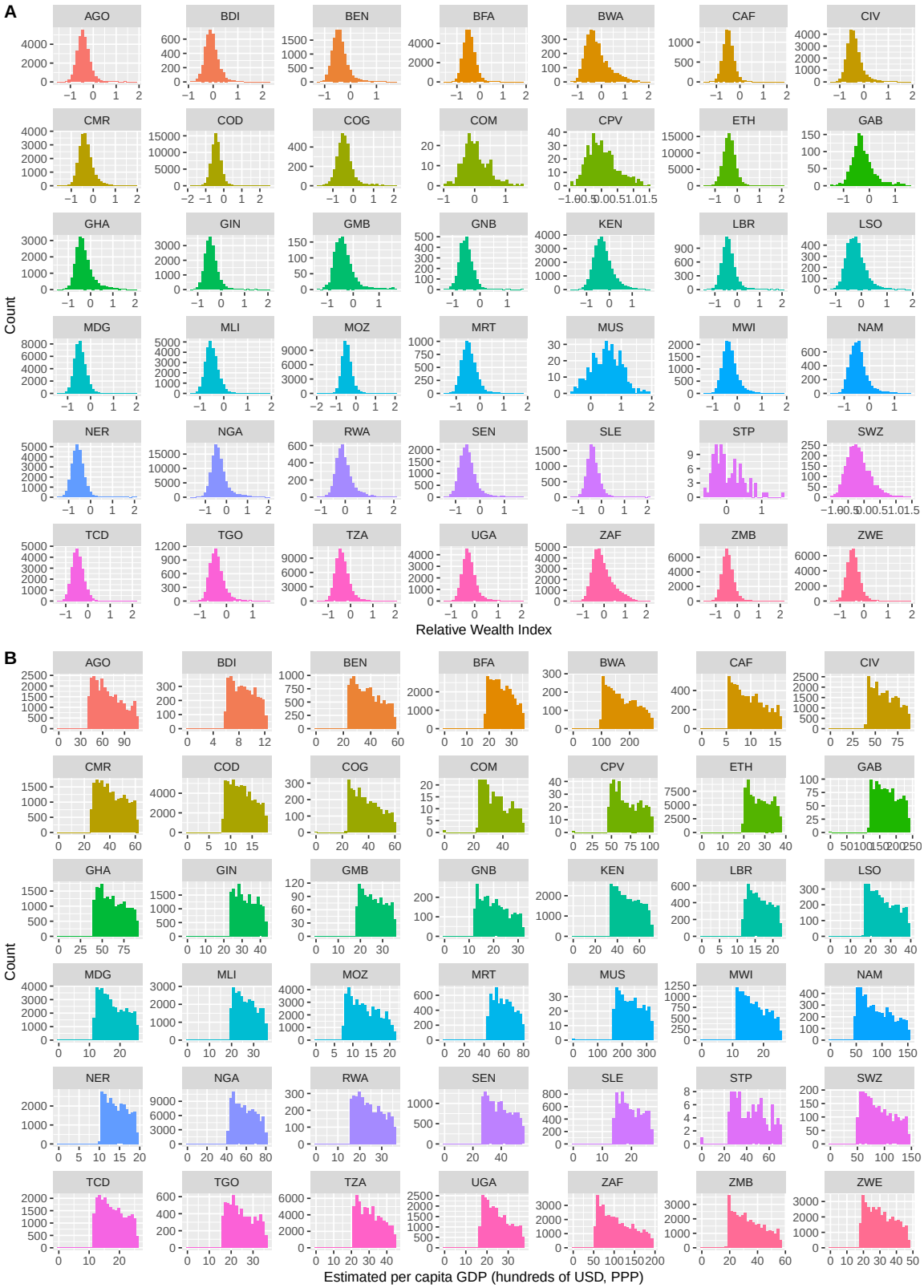

Figure SI-5. Country-level distribution of the Relative Wealth Index (RWI) and the Absolute Wealth Estimate (AWE) in PPP per-capita GDP terms.

Balancing: variables dictionary

Table SI-1. Dictionary of variables included in the balancing procedure; IDs referring to Figure 3

1	Population
2	Travel time to the nearest city
3	Distance to the capital city
4	Distance to the borders of the nearest country
5	Distance to the own national borders
6	Availability of primary (kimberlite) diamond deposits
7	Availability of secondary (alluvial) diamond deposits
8	Availability of gold deposits
9	Availability of onshore petroleum deposits
10	Availability of gems deposits
11	GAEZ agroclimatic zone
12	Malaria stability index
13	Elevation (m above the sea level)
14	Urban/rural
15	Country-level covariate: % of urban population
16	Country-level covariate: country surface area (km^2)
17	Country-level covariate: arable land (hectares per person)
18	Country-level covariate: electricity access
19	Country-level covariate: School enrollment, primary (% net)
20	Country-level covariate: renewable internal freshwater resources per capita (cubic meters)
21	Country-level covariate: ease of doing business rank
22	Country-level covariate: time required to start a business (days)
23	Country-level covariate: strength of legal rights index
24	Country-level covariate: fuel exports (% of merchandise exports)
25	Country-level covariate: ores and metals exports (% of merchandise exports)
26	Forest area
27	Country factor variable (ISO3)
28	Average precipitations (1989-2018)
29	Average temperature (1989-2018)
30	Average wetness (1989-2018)
31	spei_1_28_count_dry
32	Average precipitations (1901-2018)
33	Average temperature (1901-2018)
34	Average wetness (1901-2018)
35	spei_29_58_count_dry
36	Average precipitations (1929-1958)
37	Average temperature (1929-1958)
38	Average wetness (1929-1958)
39	spei_59_88_count_dry
40	Average precipitations (1959-1988)
41	Average temperature (1959-1988)
42	Average wetness (1959-1988)

Alternative modelling specifications: GPS via BART

In this section we provide alternative modelling specification. We use BART to estimate the GPS following the same approach described in the Materials and Methods section.

Table SI-2. Covariates balancing summary: count of variables with a correlation coefficient ± 0.05 after the balancing procedure using BART.

	Post-balancing BART			
	Dry	Dry-Extra	Wet	Wet-Extra
Balanced, <0.05	99	54	99	99
Not Balanced, >0.05	0	45	0	0

Table SI-3. GPS BART: Cumulative impact of hydrological extremes on the RWI and AWE in sub-Saharan Africa

	Dependent variable:					
	RWI (dry)	AWE (dry)	RWI (wet)	AWE (wet)	RWI (wet extreme)	AWE (wet extreme)
	(1)	(2)	(3)	(4)	(5)	(6)
Cumulative # events	-0.018^{***}	-99.189^{***}	0.004^{***}	12.368^{***}	-0.002	-146.355^{***}
	(0.0001)	(3.976)	(0.001)	(2.932)	(0.004)	(9.279)
Constant	0.962^{***}	$10,480.470^{***}$	-1.008^{***}	$1,949.068^{***}$	-0.511^{***}	$8,387.200^{***}$
	(0.000)	(0.00001)	(0.058)	(98.429)	(0.122)	(345.930)
Observations	911,430	911,430	911,430	911,430	911,430	911,430
Log Likelihood	-63,637,942.000	-71,303,373.000	-42,223,512.000	-49,158,261.000	-29,777,902.000	-36,678,487.000
Akaike Inf. Crit.	127,275,887.000	142,606,751.000	84,447,029.000	98,316,525.000	59,555,808.000	73,356,979.000

Note: *p<0.1; **p<0.05; ***p<0.01

Table SI-4. GPS BART: Time heterogeneity in the impact of hydrological extremes on the RWI and AWE in sub-Saharan Africa

	Dependent variable:					
	RWI (dry)	AWE (dry)	RWI (wet)	AWE (wet)	RWI (wet extreme)	AWE (wet extreme)
	(1)	(2)	(3)	(4)	(5)	(6)
# events (1901 - 1928)	0.165***	−587.214	0.021***	74.032***	−0.018	359.448***
	(0.041)	(462.134)	(0.003)	(9.279)	(0.039)	(99.450)
# events (1929 - 1958)	−0.018**	89.434***	−0.009**	−12.492***	0.005	−103.901***
	(0.007)	(13.976)	(0.004)	(4.570)	(0.010)	(30.279)
# events (1959 - 1988)	−0.017***	−182.581***	0.008***	−9.766**	−0.011	−172.307***
	(0.002)	(3.095)	(0.002)	(3.947)	(0.010)	(27.364)
# events (1989 - 2018)	−0.043**	−35.628	0.014***	19.711***	−0.033*	−60.275
	(0.020)	(38.182)	(0.003)	(5.152)	(0.020)	(47.979)
Constant	0.962***	10,480.470***	−1.008***	1,949.068***	0.395	5,896.841***
	(0.000)	(0.00001)	(0.058)	(98.429)	(0.579)	(1,405.316)
Observations	911,430	911,430	911,430	911,430	911,430	911,430
Log Likelihood	-63,637,942.000	-71,303,373.000	-42,223,512.000	-49,158,261.000	-29,777,900.000	-36,678,480.000
Akaike Inf. Crit.	127,275,893.000	142,606,757.000	84,447,035.000	98,316,531.000	59,555,810.000	73,356,970.000

Note: *p<0.1; **p<0.05; ***p<0.01

Quantile regressions results

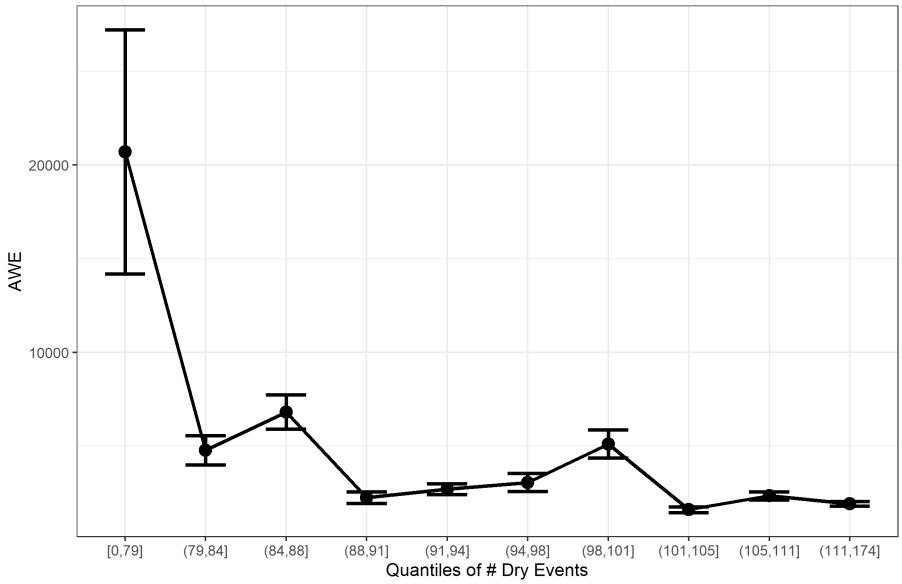

Figure SI-6. Average predicted value of AWE at each decile of the moderate dry events treatment variable (SPEI-24 < 1.5).

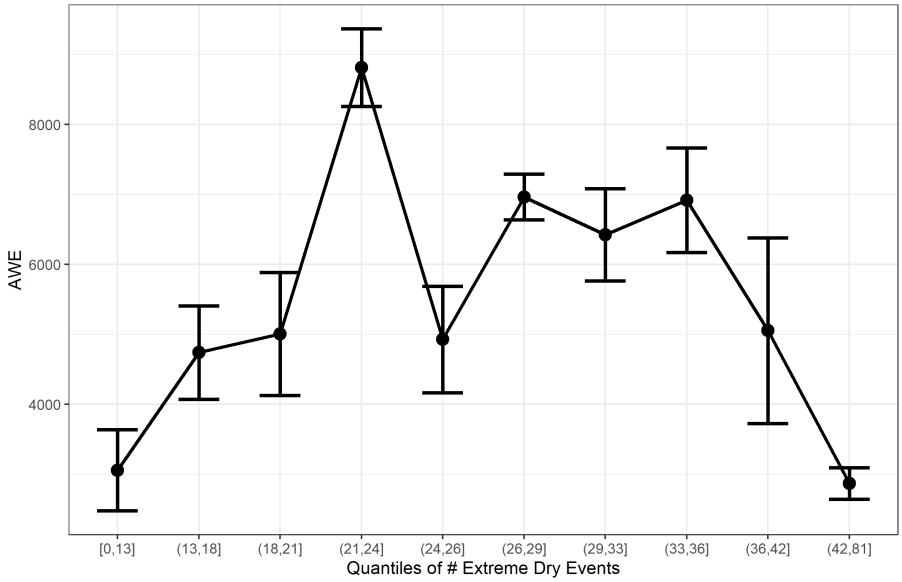

Figure SI-7. Average predicted value of AWE at each decile of the extreme dry events treatment variable (SPEI-24 < 2).

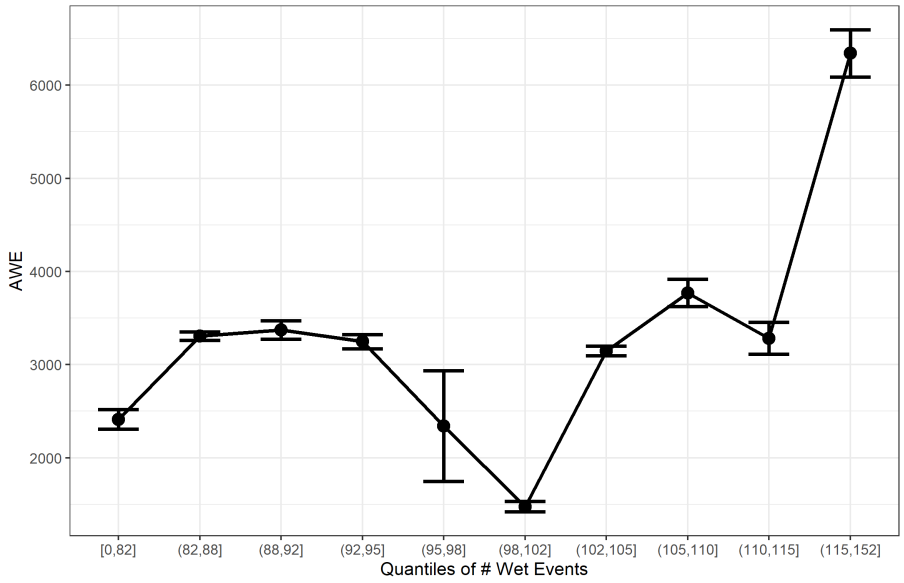

Figure SI-8. Average predicted value of AWE at each decile of the moderate wet events treatment variable (SPEI-24 $>$ 1.5).

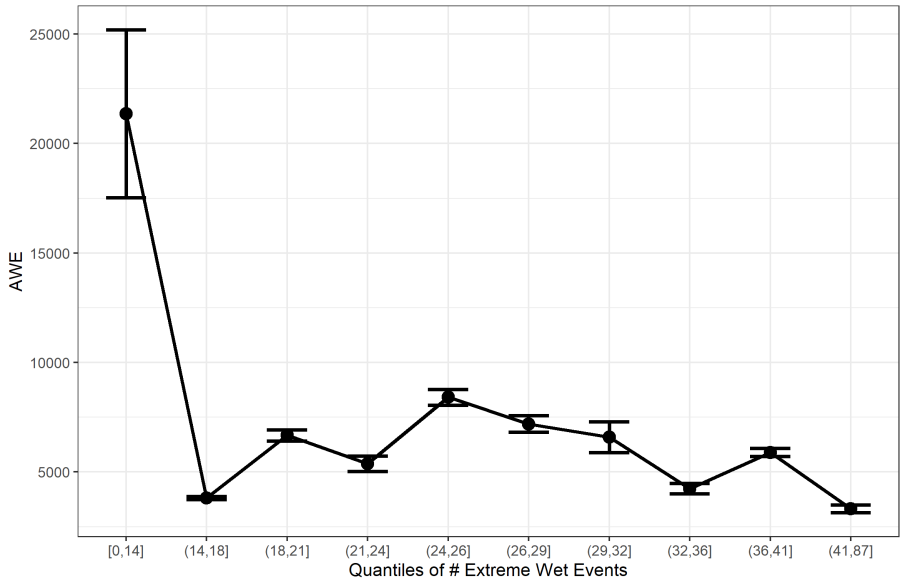

Figure SI-9. Average predicted value of AWE at each decile of the extreme wet events treatment variable (SPEI-24 $>$ 2).